

# Holographic complexity of axion-de Sitter universes

---

**Sergio E. Aguilar-Gutierrez,<sup>a</sup>**

<sup>a</sup>*Institute for Theoretical Physics, KU Leuven,  
Celestijnenlaan 200D, B-3001 Leuven, Belgium*

*E-mail:* [sergio.ernesto.aguilar@gmail.com](mailto:sergio.ernesto.aguilar@gmail.com)

**ABSTRACT:** We study the holographic complexity of a pair of asymptotically dS universes in the presence of axion matter, to characterize these observables in more general space-times. The system is prepared in a two-copy Hartle-Hawking state by slicing an Euclidean wormhole, which entangles the two universes. We derive the evolution of codimension-1 Complexity=Anything proposals by anchoring the probes to a worldline observer in each of the universes and connecting them through the Euclidean wormhole. We investigate how the axion charge competes with the cosmological constant in the time evolution of complexity. When the complexity proposal equals the volume of an extremal surface, its evolution is determined by the scale factor of the axion-dS universe, and as a result, the observable might increase nearly exponentially for low axion charge, while it decreases to a vanishing value as one approaches the maximal axion charge allowed by de Sitter space.

---

## Contents

<b>1</b>	<b>Introduction</b>	<b>1</b>
<b>2</b>	<b>Geometry of axion-de Sitter wormholes and universes</b>	<b>3</b>
2.1	Two-copy Hartle Hawking state	4
2.2	Geodesics	5
<b>3</b>	<b>C=Volume proposal</b>	<b>6</b>
3.1	$D = 3$ case	8
3.2	$Q = Q_{\max}$ case	9
<b>4</b>	<b>C=Anything proposal</b>	<b>10</b>
4.1	$D = 3$ case	12
4.2	$Q = Q_{\max}$ case	12
<b>5</b>	<b>Discussion</b>	<b>13</b>

---

## 1 Introduction

There has been much recent attention to describing quantum information observables in general backgrounds, beyond those in anti-de Sitter (AdS) space holography. One of the concepts on the frontline of these developments is holographic complexity as novel gravitational probes in general spacetimes.

Complexity in quantum mechanical systems has different definitions. One of them is circuit complexity, which refers to the minimum number of elementary gates to prepare a unitary operator or a target state from a given reference. There have been several proposals to find a holographic dual to circuit complexity in asymptotically AdS spacetimes. We will be mostly focused on codimension-1 proposals, namely complexity=volume (CV) [1, 2], and a recent generalization for codimension-1 observables, called complexity=anything (CAny) [3, 4], evaluated on codimension-1 constant mean curvature (CMC) slices [4–8]. The defining properties of the general CAny family of proposals are late-time linear growth of complexity; and the switchback effect, which describes a decrease in the growth of holographic complexity due to the appearance of energy perturbations in the geometry, motivated by epidemic growth of perturbations in quantum circuit dual models.

Much of the recent progress in studying holographic complexity beyond asymptotically AdS space, and importantly for asymptotically de Sitter (dS) space, has been made possible with the stretched horizon holography [9]. It has sparked different proposals describing

how complexity might be manifested in the static patch holography<sup>1</sup> [6–8, 11–15]. However, most of these studies have been limited to Schwarzschild-dS spacetimes. We would like to understand what these advances say about more general asymptotically dS spacetimes.

The proper way to study holographic complexity in more general dS universes can be rather unclear without static patches, as one loses the guidance of the stretched horizon to perform the anchoring of gravitational probes. However, there has been a recent (and formal) proposal [16] to study general bulk observables anchored to a worldline geodesic observer in a background-independent matter.

This approach allowed some previous work to define the notions of entropy and late-time bulk correlators in [17] for asymptotically dS universes prepared by a 2-copy Hartle-Hawking (HH) state [18], which are entangled with each other. This model consists of Einstein gravity in the presence of axion particles and a positive cosmological constant, which permits Euclidean wormhole geometries. It was originally studied in [19]. However, a proper understanding of the Euclidean geometry of this solution, and its different properties, including its interpretation in quantum cosmology, came until recently in [20], and some quantum information observables in [17]. In the Lorentzian interpretation, the pair of axion-dS universes represent spatially closed FLRW cosmologies where the axion matter is described by an ultra-stiff fluid, this means, they have an equation of state  $\rho = p$ , indicating energy density and pressure respectively. The analysis of the time direction with respect to matter inhomogeneities shows that the universes have inverted arrows of time [20] and can be interpreted as bouncing cosmologies mediated through the Wormhole. Although this class of asymptotically dS universes lacks a static patch, there has been recent work on how to recover reasonable answers with respect to entanglement entropy and bulk correlators [17]. For the approach to result in gauge invariant observables, one might resort to the late time analysis where gravity at  $\mathcal{I}^+$  of the asymptotically dS universe is weak, as in the dS/CFT holographic approach [21].

Motivated by these developments, we study the implications of anchoring complexity surfaces to geodesic worldline observers in the same background as [17]. This allows us to better understand holographic complexity for more general asymptotically dS universes that lack a static patch, and to better characterize the properties of this specific background where there is an interplay between the axion charge and the dS length scale, which determines the wormhole geometry, and in turn the entanglement between the universes. The strategy goes as follows. We locate a geodesic worldline observer in each of the universes equipped with a clock that has been previously synchronized. They will measure the CV and CAny proposals as a function of global time. To fully specify the system, we require a second boundary condition determining how the extremal complexity surfaces extend in the spacetime. We will require that they intercept with the Euclidean wormhole in the past of each observer and that the complexity proposals are maximal at the location where the interception occurs. Our results show that the time evolution of the complexity proposals increases exponentially in terms of the global time of the FLRW cosmologies. Alternatively, it can also decrease and reach a

---

<sup>1</sup>See [10] for a recent review.

constant value for a sufficiently large axionic charge. The modification in the behaviors of the complexity proposals depending on the axion charge is related to the expansion rate of the universes, given by the evolution of the scaling factors.

**Structure:** In Sec. 2 we provide a lightning review about the axion-dS universes. In Sec. 3 we study the CV proposal. We emphasize the role of anchoring complexity extremal surfaces to the observer, how they would connect with the Euclidean wormhole, and discuss the effects of the axion charge on the evolution of the complexity proposals. In Sec 4, we investigate the CAny proposal using CMC slices as evaluation regions for the codimension-1 observables, and the resulting modification on the rate of growth as the mean curvature increases. Finally, Sec. 5 includes a summary of the manuscript and some future directions.

## 2 Geometry of axion-de Sitter wormholes and universes

In this section, we briefly review the properties of axion-dS universes, which are prepared from an Euclidean wormhole. More geometric details can be found in [20] as well as some results on the on-shell action of these solutions and their perturbative stability; while a discussion about entanglement and late-time bulk correlators in the Lorenzian theory is given in [17].

Our starting point is  $D$ -dimensional Euclidean Einstein gravity in the presence of axion matter content and a positive cosmological constant:

$$I = \int \left[ -\frac{1}{2\kappa_D^2} \star (R - 2\Lambda) + \frac{1}{2} \star H_{D-1} \wedge H_{D-1} \right], \quad (2.1)$$

where  $H_{D-1}$  is the axion flux field, which is Hodge dual to the axion field  $\chi$  (i.e.  $H_{D-1} = \star d\chi$ );  $\kappa_D^2 = 8\pi G_N$  and we will consider a cosmological constant

$$\Lambda = \frac{(D-1)(D-2)}{2L^2} > 0. \quad (2.2)$$

The presence of the axion flux field in (2.1) produces Strominger-Giddings wormhole [22]-type of solutions. One can study them by considering spherical symmetric solutions for this theory:

$$ds^2 = N(\tau)^2 d\tau^2 + a(\tau)^2 d\Omega_{D-2}^2, \quad (2.3)$$

where we denote

$$d\Omega_{D-1}^2 = d\theta_1^2 + \cos^2 \theta_1 d\theta_2 + \dots + \cos^2 \theta_1 \dots \cos^2 \theta_{D-2} d\theta_{D-1}^2, \quad (2.4)$$

with  $\theta_i \in [-\frac{\pi}{2}, \frac{\pi}{2}]$  when  $1 < i < D-2$ , and  $\theta_{D-1} \in [0, 2\pi]$ .

The Lorenzian Einstein equations from (2.1) reduce to the constraint

$$\left( \frac{1}{N(\tau)} \frac{da}{d\tau} \right)^2 = 1 - \frac{a^2}{L^2} - \frac{\kappa_D^2 Q^2 a^{-2(D-2)}}{(D-1)(D-2)}. \quad (2.5)$$

where the parameter  $Q$  is a Noether charge of (2.1) associated with constant shifts in the axion field  $\chi$  ( $H_{D-1} := \star d\chi$ ),  $\chi \rightarrow \chi + \zeta$  with  $\zeta \in \mathbf{R}$ . It can be seen from the roots in

(2.5) that  $a(\tau)$  will always reach the same minimum and maximum values,  $a_{\min}$  and  $a_{\max}$  respectively, for any choice of the gauge parameter  $N(\tau)$ . To study the global geometry, we will consider the gauge choice  $N(\tau) = 1$  from this point onward.

Moreover, the axion charge cannot take arbitrary values; there is a bound on the maximal size for the wormholes preparing the state, denoted by “*Nariai wormhole*”, which can be obtained by extremizing (2.9) with respect to the scale factor  $a$ ,

$$\kappa_D^2 Q_{\max}^2 = L^{2(D-2)} (D-2) \left( \frac{D-2}{D-1} \right)^{D-2}. \quad (2.6)$$

In this limit, the scale factor is a constant, given by

$$a_N := a_{\max}(Q_{\max}) = a_{\min}(Q_{\max}) = \sqrt{\frac{D-2}{D-1}} L. \quad (2.7)$$

## 2.1 Two-copy Hartle Hawking state

Our main interest is studying the real time evolution of complexity observables for these geometries, so we will now discuss the Lorentzian continuation, found by a simple Wick rotation  $\tau \rightarrow i t$  in the global coordinate system (corresponding to the gauge choice  $N(t) = 1$ ):

$$ds^2 = -dt^2 + a(t)^2 d\Omega_{D-1}^2, \quad (2.8)$$

$$\left( \frac{da}{dt} \right)^2 = -1 + \frac{a^2}{L^2} + \frac{\kappa_D^2 Q^2 a^{-2(D-2)}}{(D-1)(D-2)}. \quad (2.9)$$

One can generate the Lorentzian geometry as a two-copy HH state preparation by slicing the wormhole at either  $a = a_{\max}$  or  $a = a_{\min}$ , and performing the Wick rotation. The careful analysis of the scale factor in Lorentzian signature [20] reveals that if one does this slicing at  $a_{\max}$ , we generate an expanding universe dominated by the cosmological constant term  $\Lambda$ ; while the slicing for  $a_{\min}$  leads to the contracting branch, due to the high density of axion matter. We will focus on the first choice, illustrated in Fig. 1, so that the resulting universes have dS asymptotics, and allow for a late-time evolution of gravitational observables, as well as a notion of weak gravity near  $\mathcal{I}^+$ . Moreover, by studying the propagation of matter inhomogeneities, one can find that the arrow of time [23] follows opposite directions between the two universes, as we have illustrated in Fig. 1.

For much of the following discussion, we will need the behavior of  $a(t)$  in (2.9). For general values of  $Q$ , there are no analytic expressions for the scaling factors in this gauge. Numerical results in  $D = 4$  are shown in Fig. 2.

For convenience, one can consider the  $D = 3$  in (2.9) where we can find analytic solutions for  $a(\tau)$  in (2.8):

$$ds^2 = -dt^2 + \frac{L^2}{2} \left( 1 + \cosh\left(\frac{2t}{L}\right) \sqrt{1 - \mu^2} \right) d\Omega_2^2, \quad (2.10)$$

$$\mu := \frac{Q}{Q_{\max}}. \quad (2.11)$$

Identifying the allowed range to cover the entire geometry, one sees that in this coordinate system  $\tau \sim \tau + \pi/L$ .

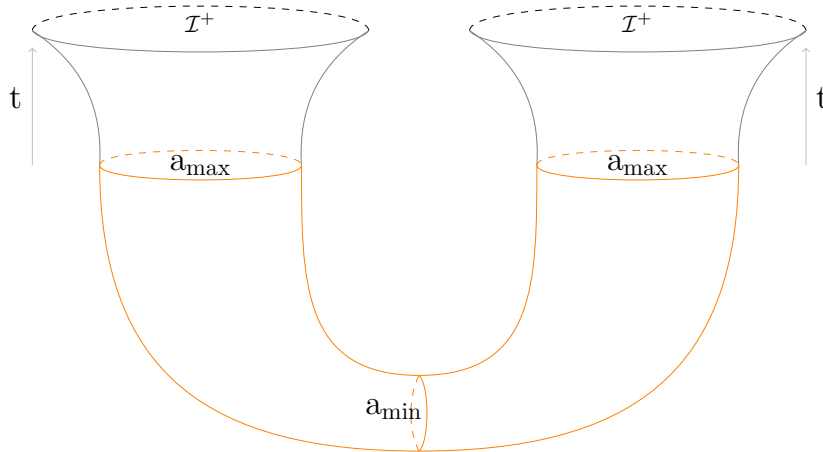


**Figure 1.** Preparation of the pair of axion-dS universes (gray surface) by slicing an Euclidean wormhole (orange surface) and performing the Wick rotation to global time  $t$  in (2.8), which generates a two-copy HH state preparation. We illustrate the procedure by doing the continuation maximum scale factor  $a_{\max}$ , while  $a_{\min}$  represents the throat of the wormhole. This procedure results in expanding asymptotically dS universes

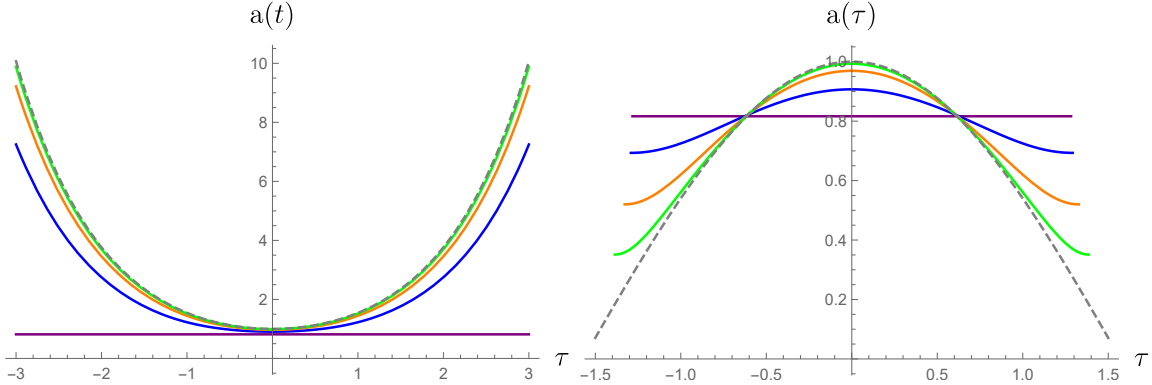


**Figure 2.** Scale factors in the regular global metric (2.8) with  $D = 4$  in Lorentzian (*left*) and Euclidean (*right*) signature (where  $\tau = it$ ) for different values of the parameter  $\mu := Q/Q_{\max}$ ;  $\mu = 1$  (purple), 0.9 (blue), 0.6 (orange) and 0.3 (green), and 0 (dashed gray) corresponding to pure dS space. All curves have  $L = 1$ .

## 2.2 Geodesics

Lastly, we would like to identify geodesic trajectories in this background geometry. It can be shown that for each of the axion-dS universes, there is a unique geodesic passing through the wormhole at  $\theta_i(\tau = \tau_{\max}) = 0$ , corresponding to [17]

$$\theta_i^{(g)}(t) = 0, \quad 1 \leq i \leq D - 1, \quad t \geq 0 \quad (2.12)$$

is the only solution to the geodesic equations respecting the boundary conditions. This fact will prove useful when we consider gravitational probes anchored to a pair of worldline

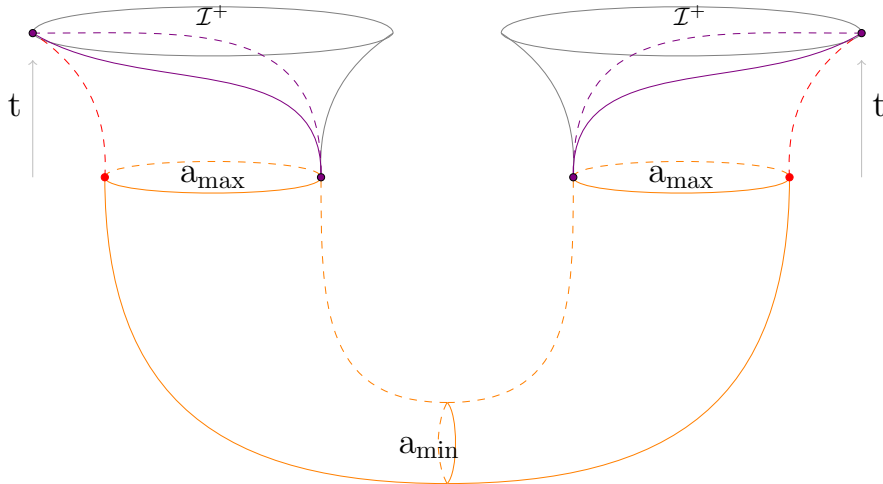


**Figure 3.** Proposal for evaluating maximal codimension-1 volume surfaces (purple surfaces) anchored to pairs of worldline observer following the geodesic  $\theta_i^{(g)}(t) = 0$  (red dashed lines) in axion-dS universes connected through an Euclidean axion wormhole (orange surface).

observers.

### 3 C=Volume proposal

The C=Volume (CV) [1, 2] proposal is defined as

$$\mathcal{C}_V(\Sigma) = \max_{\Sigma=\partial\mathcal{B}} \frac{V(\mathcal{B})}{G_N l} \quad (3.1)$$

where  $\Sigma$  is a time slice,  $G_N$  Newton's constant;  $l$  an arbitrary length scale, which we will take to be the dS radius  $L$ ; and  $\mathcal{B}$  a bulk hypersurface anchored at  $\Sigma$ , with a corresponding volume  $V(\mathcal{B})$ .

While we look for codimension-1 surfaces anchored to the geodesics in (2.12), given the symmetries of the problem, the spatial dependence on the extremal surface will only depend on one of the polar angles,  $\theta_1$  in (2.4). For this reason, from now on, we will denote  $\theta_1 \equiv \theta$  for notational convenience. The setting is illustrated in Fig. 3.

The complexity=volume proposal (3.1) for (2.8) then leads to

$$\mathcal{C}_V = \frac{1}{G_N L} \int d\Omega_{D-2} \int d\lambda \sqrt{-(t'(\lambda))^2 + a(t)^2 (\theta'(\lambda))^2} a(t)^{D-2} \cos^{D-2} \theta, \quad (3.2)$$

where primes indicate differentiation. Notice that in this functional we do not account for the volume of the Euclidean wormhole coupling the universes, as we are concerned with the time dependence of holographic complexity.

Notice that there are no conserved charges for the functional above; we would need to solve for the extremal complexity surfaces  $(\theta(\lambda), t(\lambda))$  described by a non-linear coupled

system of second-order ordinary differential equations, given by

$$0 = a(t) \cos(\theta) (a'(t)\theta'(\lambda) ((D-1)a(t)^2\theta'(\lambda)^2 - Dt'(\lambda)^2) + a(t) (\theta'(\lambda)t''(\lambda) - \theta''(\lambda)t'(\lambda))) \\ + (D-2) \sin(\theta)t'(\lambda) (t'(\lambda)^2 - a(t)^2\theta'(\lambda)^2) , \quad (3.3)$$

$$0 = a(t) \cos(\theta) (\theta'(\lambda)a'(t(\lambda)) ((D-1)a(t)^2\theta'(\lambda)^2 - Dt'(\lambda)^2) + a(t) (\theta'(\lambda)t''(\lambda) - \theta''(\lambda)t'(\lambda))) \\ + (D-2) \sin(\theta)t'(\lambda) (t'(\lambda)^2 - a(t)^2\theta'(\lambda)^2) . \quad (3.4)$$

To simplify the evaluation, one needs to find an appropriate gauge choice for  $\lambda$  where to implement the boundary conditions most conveniently. Given that we anchor the surfaces to a pair of worldline observers along  $\theta = 0$  in each of their universes, and we require that these surfaces connect the two observers through the Euclidean wormhole, as shown in Fig. 3. Therefore, we impose the following boundary conditions:

$$t(\theta = 0) = t_{\text{obs}} , \quad t \left[ \theta = \frac{\pi}{2} \right] = 0 , \quad (3.5)$$

where  $t_{\text{obs}}$  is the physical time for the geodesic observers, for which we choose to synchronize their clocks for simplicity. As for the second equality in (3.5), this represents that the complexity surfaces anchored to the worldline observer will always reach the Euclidean wormhole (see Fig. 3) coupling the two universes at  $t(\theta) = 0$ , which is maximal for  $\theta = \pi/2$  when the observers are located at  $\theta = 0$ , given that  $\theta \in [-\pi/2, \pi/2]$  and the argument of the integral (3.2) is positive definite over this range, as made manifest in the  $\lambda = \theta$  gauge.

Also note that, given that the choice of boundary conditions (3.5) relies on having a Euclidean wormhole coupling the pair of universes, the proposal does not apply for the pure dS space limit where the axion charge  $Q = 0$ .

Therefore, we proceed using the  $\lambda = \theta$  gauge where the boundary conditions (3.5) can be most conveniently implemented, such that (3.2) becomes:

$$\mathcal{C}_V = \frac{\Omega_{D-2}}{G_N L} \int_0^{\pi/2} d\theta \mathcal{L}_V , \quad (3.6) \\ \mathcal{L}_V := \sqrt{-(t'(\theta))^2 + a(t)^2} a(t(\theta))^{D-2} \cos^{D-2} \theta .$$

The equations of motion for the complexity surface from  $\mathcal{C}_V$  can be expressed as:

$$0 = \cos(\theta)a(t(\theta)) (a'(t(\theta)) ((D-1)a(t(\theta))^2 - D t'(\theta)^2) + a(t(\theta))t''(\theta)) \\ + (D-2) \sin(\theta)t'(\theta) (t'(\theta)^2 - a(t(\theta))^2) . \quad (3.7)$$

Lastly, we can explicitly check that the choice of boundary conditions (3.5) is compatible with the extermination procedure for the functional  $\mathcal{C}_{\text{CMC}}$  (4.2). First notice that for the total variation  $\delta\mathcal{C}_V$  to vanish after imposing the equation of motion in (4.5) requires that:

$$\delta t(\theta)a(t(\theta))^{D-2} \cos^{D-2} \theta \frac{t'(\theta)}{\sqrt{-(t'(\theta))^2 + a(t(\theta))^2}} \Big|_{\theta=0}^{\theta=\pi/2} = 0 . \quad (3.8)$$



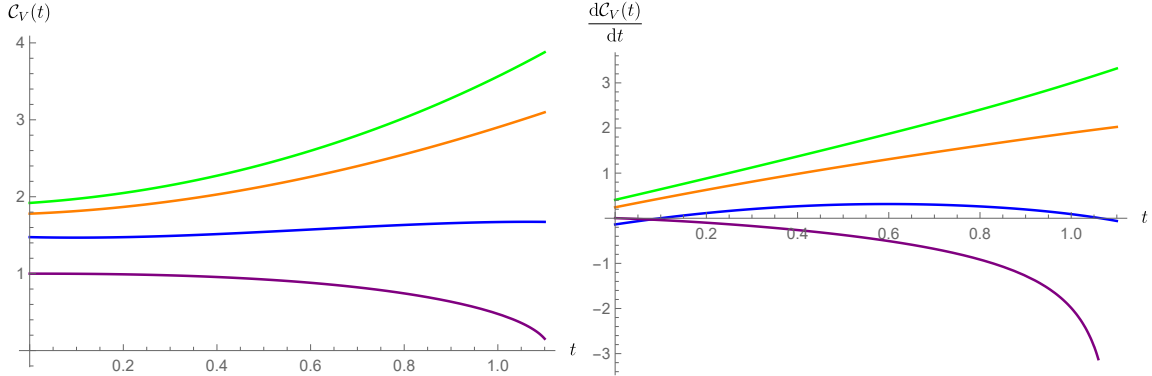


**Figure 4.** *Left:* Complexity growth of the axion-dS universes in  $D = 3$  according to the CV conjecture, and *Right:* its rate of growth for different values of  $\mu = 1$  (purple), 0.9 (blue), 0.6 (orange) and 0.3 (green). Other parameters:  $G_N = 1$  and  $L = 1$ .

This condition is satisfied with (3.5) since we have Dirichlet boundary conditions at  $\theta = 0$ , while the term at  $\theta = \pi/2$  necessarily vanishes for  $D > 2$ .

Next, we will explicitly study the evolution of the CV proposal. Since  $a(t)$  in (2.8) is only known analytically for  $D = 3$  with arbitrary  $Q \leq Q_{\max}$ , and when  $Q = Q_{\max}$  in arbitrary  $D$ , we will focus in these cases. However, the implementation should be valid for more arbitrary cases.

### 3.1 $D = 3$ case

We now solve numerically the complexity surfaces  $t(\theta)$  in (3.7) with (3.5) for the  $D = 3$  axion-dS scale factor (2.10) and substitute in the proposal (3.6). Fig. 4 shows the evolution of the CV complexity.

The plot 4 is presented for  $t \sim \mathcal{O}(1)$   $L$  the numerical results become noisy at late times. However, in order for these observables to be evaluated in a weak gravitate regime, one should study the late time regime. We confirmed (albeit in the presence of noise) that the late-time behavior follows a similar trend, CV is nearly exponentially increasing for different charge ratios ( $\mu = 0.3, 0.6$  in the plot). The reason for this is encoded in the scale factors (2.10), which are nearly exponentially increasing at late time. Since the complexity surfaces are anchored between the worldline observers  $\theta = 0$  and the wormhole  $t(\theta = \pi/2) = 0$ , the time dependence encoded in the scale factor (3.6) allows for the volumes to reach large late-time values.

However, this issue is more subtle as there is also competition with the axion density. When the parameter  $\mu \sim 1$ , CV transitions to a decaying behavior, particularly in the Nariai limit ( $\mu = 1$ ), where it decreases it vanishes at a finite time scale. This situation is analyzed in more detail in the following subsection.

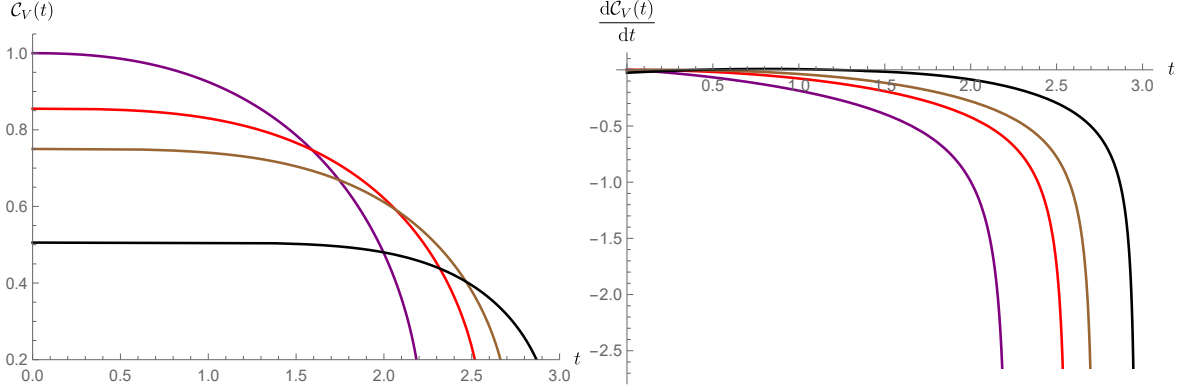


**Figure 5.** *Left:* Complexity growth of the axion-dS universes in the Nariai limit ( $\mu = 1$ , corresponding to a pair of Einstein static universes) according to the CV conjecture, and *Right:* its rate of growth for  $D = 3$  (purple), 4 (red), 5 (brown) and 10 (black). The maximal volume decreases over time. Other parameters:  $G_N = 1$  and  $L = 1$ . Range of integration in (3.10, 3.11).

### 3.2 $Q = Q_{\text{max}}$ case

As we saw in (2.7), the scale factor is a constant  $a_N = \sqrt{\frac{D-2}{D-1}}L$ . We can then write the conserved charge for (3.6) as

$$\begin{aligned}
 P &= \frac{d\mathcal{L}_V}{dt'(\lambda)} \\
 &= -\frac{a_N^{D-2} \cos^{D-2} \theta t'(\lambda)}{\sqrt{-(t'(\lambda))^2 + a(t)^2(\theta'(\lambda))^2}}.
 \end{aligned} \tag{3.9}$$

One can then find integral expressions for:

$$C_V = \frac{1}{G_N L} \int_0^{\pi/2} \frac{a_N^{2D-3} \cos^{2(D-2)} \theta d\theta}{\sqrt{P^2 + a_N^{2(D-2)} \cos^{2(D-2)} \theta}}, \tag{3.10}$$

$$t_{\text{obs}} = -\int_0^{\pi/2} \frac{P a_N d\theta}{\sqrt{P^2 + a_N^{2(D-2)} \cos^{2(D-2)} \theta}}. \tag{3.11}$$

The cases  $D = 3, 4, 5$  and 10 are plotted in Fig. 5.

As we saw in Sec. 3.1, the CV proposal seems to decrease in time until it reaches a vanishing value. The analysis of integrals above (3.10) and (3.11) shows that the complexity evolution cannot take place indefinitely,  $t_{\text{obs}}$  can be at most  $t_{\text{crit}} := \frac{\pi}{2} a_N$ , so the time evolution of these surfaces stops, which coincides when  $C_V$  reaches 0 for  $P$  large enough. The reason for this is related to the scale factor being constant. There are no longer extremal surfaces obeying the boundary conditions (3.5) once we reach the critical time  $t_{\text{crit}}$ , and as a result, there is no longer an appropriate measure of codimension-1 volume. We will explore how this situation is modified with the CAny proposal in Sec. 4.2.

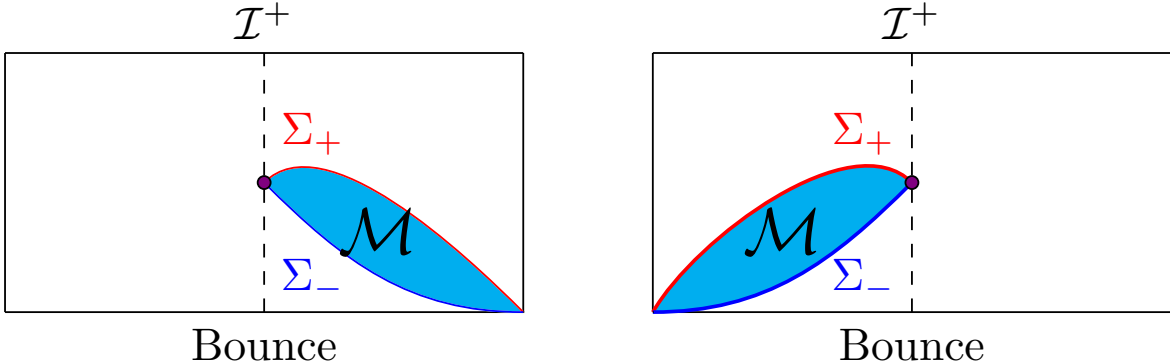


**Figure 6.** Proposal for evaluating the volume of CMC slices for axion-dS universes connected through a quantum bounce (corresponding to the Euclidean wormhole in Fig. 1, and explained in Sec. 1). We anchor codimension-one extremal complexity surfaces  $\Sigma_-$  and  $\Sigma_+$  (in blue and red respectively) to worldline geodesic observers (represented by black dashed lines), which form the past and future boundaries of the spacetime region  $\mathcal{M}$ , where  $\mathcal{C}^\epsilon$  in eq. (4.1) is evaluated. The observers measure their proper time. The precise profile of the  $\Sigma_\pm$  slices is determined by the extremization of eq. (4.2).

We remark that the Nariai limit is not asymptotically dS, as one notices by the fact that the scale factor is a constant; its Lorentzian interpretation is that of a pair of Einstein static universes that are coupled to one another through the Euclidean wormhole. The results are meant to provide a better analytic understanding of the late-time behavior of the axion-dS universes where  $\mu \sim 1$ .

#### 4 C=Anything proposal

We are interested in codimension-one observables within the class of the complexity=anything proposal [3–5]. First, we define the set of codimension-1 holographic complexity as the physical observable

$$\mathcal{C}^\epsilon \equiv \frac{1}{G_N L} \int_{\Sigma_\epsilon} d^{D-1} \sigma \sqrt{h} F[g_{\mu\nu}, \mathcal{R}_{\mu\nu\rho\sigma}, \nabla_\mu], \quad (4.1)$$

where  $F[g_{\mu\nu}, \mathcal{R}_{\mu\nu\rho\sigma}, \nabla_\mu]$  is an arbitrary scalar functional of  $D$ -dimensional bulk curvature invariants of the bulk region  $\mathcal{M}$ , which is covariantly defined by extremizing a combination of codimension-one and codimension-zero volumes with different weights, given by

$$\mathcal{C}_{\text{CMC}} = \frac{1}{G_N L} \left[ \alpha_+ \int_{\Sigma_+} d^{D-1} \sigma \sqrt{h} + \alpha_- \int_{\Sigma_-} d^{D-1} \sigma \sqrt{h} + \frac{\alpha_B}{L} \int_{\mathcal{M}} d^D x \sqrt{-g} \right] \quad (4.2)$$

where  $\Sigma_\pm$  are the future (past) boundaries of  $\mathcal{M}$  anchored at the locations in (3.5), such that  $\partial\mathcal{M} = \Sigma_+ \cup \Sigma_-$ , as shown in Fig. 6.<sup>2</sup>

We denote with  $h$  the determinant of the induced metric on  $\Sigma_\pm$ . The coefficients  $\alpha_\pm$  and  $\alpha_B$  are dimensionless positive constants, therefore the extremization of the functional (4.2)

<sup>2</sup>We will label with  $\epsilon = +, -$  the quantities defined on the codimension-one surfaces  $\Sigma_\pm$ .

defines constant mean curvature (CMC) slices, for which the extrinsic curvature is given by [4, 24]

$$K_\epsilon := K \Big|_{\Sigma_\epsilon} = -\epsilon \frac{\alpha_B}{\alpha_\epsilon L}, \quad (4.3)$$

where we consider outward-pointing vectors with respect to the surfaces  $\Sigma_\epsilon$  to be future-directed.

We now perform the explicit evaluation of (4.1) using the explicit background geometry (2.8, 2.9), using the same boundary conditions in (3.5):

$$\mathcal{C}^\epsilon = \frac{\Omega_{D-2}}{G_N L} \int d\theta \sqrt{-(t(\theta))^2 + a(t)^2} b(t) a(t)^{D-2} \cos^{D-2} \theta, \quad (4.4)$$

where  $b(t)$  is an arbitrary function corresponding to the choice of the functional  $F[\dots]$  in (4.1) for the background (2.8).

Meanwhile, we can evaluate the contribution of the spacetime volume and codimension-1 volumes of  $\Sigma_\pm$  in (4.2) with (2.8, 2.9), which leads to

$$\mathcal{C}_{\text{CMC}} = \sum_\epsilon \frac{\alpha_\epsilon \Omega_{D-1}}{G_N L} \int_{\Sigma_\epsilon} d\theta \left[ \sqrt{-(t(\theta))^2 + a(t)^2} a(t)^{D-2} + K_\epsilon \int dt a(t)^{D-1} \right] \cos^{D-2} \theta \quad (4.5)$$

with  $K_\epsilon$  given in (4.3).

Next, we need to extremize (4.5) to find the complexity surfaces  $t(\theta)$ . First, notice that the argument about the boundary conditions in (3.5) is still consistent with the extremization of (4.2), since for the total variation to vanish  $\delta\mathcal{C}_{\text{CMC}} = 0$  after imposing equations of motions (4.6), one requires the exact same condition in (3.8). This means that the parameter  $K_\epsilon$  does not change the argument that we gave in Sec. 3.

Next, notice that there is no longer a conserved momentum associated with the global time  $t(\theta)$ , instead the equations of motion for (4.5) read:

$$\begin{aligned} 0 = & \cos(\theta) a(t(\theta))^3 \left( (D-1) a'(t(\theta)) + K_\epsilon \sqrt{a(t(\theta))^2 - t'(\theta)^2} \right) \\ & - \cos(\theta) a(t(\theta)) t'(\theta)^2 \left( D a'(t(\theta)) + K_\epsilon \sqrt{a(t(\theta))^2 - t'(\theta)^2} \right) \\ & + a(t(\theta))^2 \left( (2-D) \sin(\theta) t'(\theta) + \cos(\theta) t''(\theta) \right) + (D-2) \sin(\theta) t'(\theta)^3 \end{aligned} \quad (4.6)$$

where the boundary conditions are the same as those in (3.5), given that we still consider anchoring gravitational probes to the worldline observers in Fig. 3.

A technical issue in the evaluation of (4.6) is that, as we have explained in Sec. 2, the scale factor in the global metric needs to be determined by numerical methods for general charge ratio  $\mu := Q/Q_{\text{max}}$  in higher dimensions.

As discussed in Sec. 3, the scale factor  $a(t)$  in the regular global metric (2) needs to be found numerically, which complicates the evaluation for the EOM (4.6). To properly illustrate the procedure, we will work with the exactly solvable cases for  $a(t)$ , namely  $D = 3$  with  $0 \leq \mu \leq 1$  arbitrary (2.10), and for  $\mu = 1$  with  $D$  arbitrary (2.7). We expect similar results to hold  $D = 4$  and arbitrary  $0 < \mu \leq 1$ .

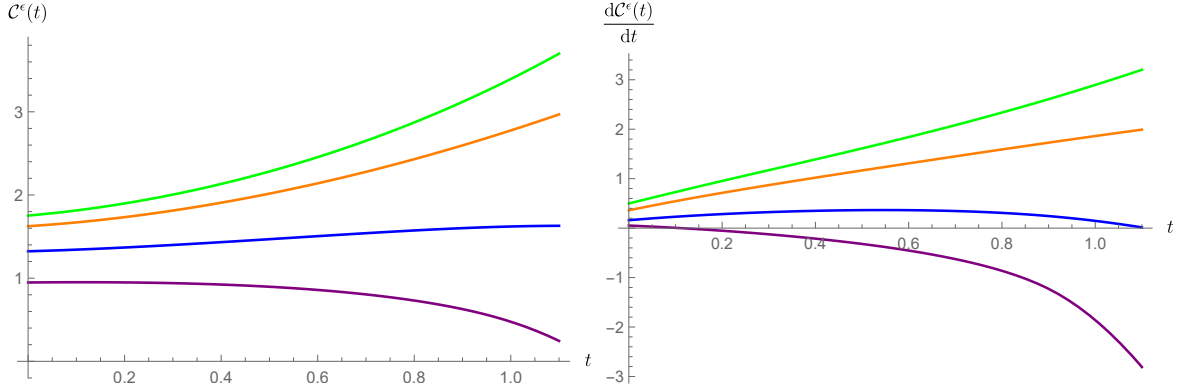


**Figure 7.** Holographic complexity (*left*) and its rate of growth (*right*) according to the CAny proposal evaluated with CMC slices (4.5). The parameters are the same as displayed in Fig. 4, with the addition of  $K_- = 1/L$  and  $F[\dots] = 1$ . The rate of growth is increased with respect to that in the CV proposal in Fig. 4.

#### 4.1 $D = 3$ case

We will perform a numerical analysis similar to that in Sec. 3.1. Using the scale factor in (2.10) in the EOM (4.6) subject to the boundary conditions (3.5) leads to the complexity surfaces  $t(\theta)$  that can be inserted in the CAny proposal. The results when  $F[\dots] = 1$  (4.1) (corresponding to  $b(t) = 1$  in (4.4)) are displayed in Fig. 7.

The evolution of the proposal is very similar to the findings in Sec. 4 for the CV proposal, for which  $K_\epsilon = 0$ . The difference is in the rate of growth that increases. This happens given that the CMC slices tilt towards the past as  $K_- > 0$  is increased; so that they increase in size as the worldline observer moves towards the future in asymptotically dS space. This allows for the increased rate of growth of codimension-1 volumes evaluated on the CMC slices. In contrast, we would recover a decrease in the rate of growth with respect to the CV case when using  $K_+$ , which is negative as seen in (4.3).

#### 4.2 $Q = Q_{\max}$ case

First, notice that although in the  $Q = Q_{\max}$  regime  $a(t) = a_N$  is a constant, there is still  $t(\theta)$  dependence in the functional (4.5), and as a result, there would no be conserved charges for  $\mathcal{C}_{\text{CMC}}$ , unlike in Sec. 3.2. Thus, we will proceed with the numerical analysis as in the previous subsection.

We solve the EOM (4.6) with the scale factor (2.7) and the boundary conditions (3.5). The resulting evolution for the CAny CMC proposal is displayed in Fig. 8.

The results are reminiscent of those we found in Sec. 3.2. Namely, there is a critical time,  $t_{\text{crit}}$ , for which the complexity surface no longer exists for the set of boundary conditions in (3.5). However, we see that by increasing the value of  $K_\epsilon$  ( $\epsilon = -$  in Fig. 8), it takes longer

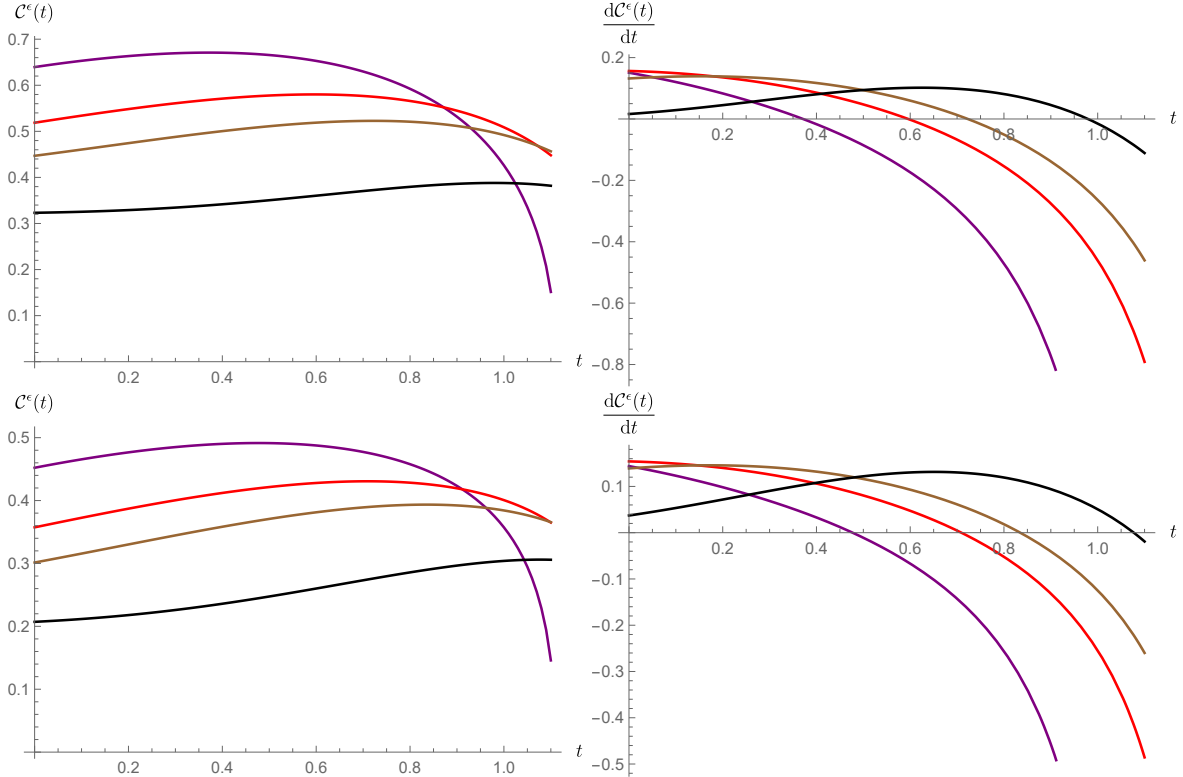


**Figure 8.** Holographic complexity (*left*) and its rate of growth (*right*) according to the CAny proposal evaluated with CMC slices (4.2), with  $K_- = 5/L$  (above), and  $K_- = 10/L$  (below). The other parameters are the same as displayed in Fig. 5, and  $F[\dots] = 1$ . We notice that as  $K_-$  is increased, the rate of growth of  $C^\epsilon$  at given  $t$  is also increased.

for  $C^\epsilon$  to decrease, indicating that the  $t_{\text{crit}}$  can be prolonged by properly increasing  $K_\epsilon$ . It would be interesting to find if there is an asymptotic regime where  $t_{\text{crit}} \rightarrow \infty$ .

## 5 Discussion

To summarize, we have investigated holographic complexity in axion-dS universes, which describe spatially closed bouncing FLRW cosmologies with an ultra-stiff fluid (with an equation of motion  $\rho = p$ ) that are coupled through a Euclidean wormhole. We focused on the case where these cosmologies have dS asymptotics. We allowed for a worldline geodesic observer to reside in each universe and studied how the CV and CAny observables evolve when they are anchored to the observers and pass through the Euclidean wormhole connecting the universes. Our results show that generically these proposals evolve with a nearly exponential dependence on the observer's time if the axion charge is low enough and that the evolution can instead decrease when the axion charge approaches the maximal value allowed by dS space, which is referred to as the Nariai limit. The main results are shown in Figs. 4, 5, 7, 8.

While our analysis for the CAny observables was focused on the volume of the CMC slices. However, since  $b(t)$  in (4.4) is an arbitrary function, it can modify significantly the behavior for other choices from  $b(t) = 1$  that we took. However, since this parameter does not enter the equations of motion for the extremal complexity surfaces, it would not change the fact that there are complexity surfaces that no longer exist after a critical time  $t_{\text{crit}}$  in Sec. 4.2.

There were certain limitations in the numerical part of the work which we comment on below.

First, the analysis of the time dependence was performed for  $t \sim \mathcal{O}(1) L$  given the limitations in the numerical integration at late times, where more noise is introduced. However, we observed (up to numerical noise) that they still follow an exponentially increasing behavior.

Second, as we mentioned in the main text, we focused on solving  $D = 3$  for any value  $Q$ ; and the  $Q = Q_{\text{max}}$  limit; this was purely for numerical and analytic convenience, given that the numerical methods for solving (4.6) need further improvement elaboration when  $a(t)$  in the global coordinate system (2.8) is only known numerically. Given that the scale factors in  $D = 4$  do not change significantly with respect to the  $D = 3$  case, we suspect our results for the time evolution of codimension-1 complexity proposals would be very similar in that case.

Third, regarding the transition between increasing or decreasing complexity, we found numerically that it happens when the charge ratio is around  $\mu \approx 0.9$ . The exact value where this transition appears would require a better numerical implementation for the late-time behavior. It would be interesting to investigate some analytic approaches for determining it.

We now comment on future avenues for investigation.

First, the fact that we study holographic complexity proposals for entangled universes is reminiscent of recent work on Nielsen complexity for bipartite quantum systems [25]. It would be interesting to further relate our works, perhaps with a holographic dual theory near  $\mathcal{I}^+$ .

Secondly, related to the increase versus decrease in complexity depending on the axion charge, according to Nielsen's geometric approach to circuit complexity [26–28] its growth should not be greater than linear [29]. This might imply that our findings represent something closer to Krylov complexity for the putative microscopic theory, conjectured to be located near  $\mathcal{I}^+$ . It would be important to develop a better understanding of the microscopic interpretation with an appropriate quantum circuit model.

Thirdly, our work has been focused on the codimension-1 holographic complexity CAny proposals. However, there is a larger class of codimension-0 CAny proposals [3]. It would be interesting to study how generic our finding about the increase and decrease of complexity is affected by the axion charge.

Moreover, our approach to holographic complexity in axion-dS universes assumes a pair of geodesic observers to anchor gravitational probes; this is fundamentally different from the stretched horizon approach to dS complexity, initiated in [11]. We hope this study provides new insights into holographic complexity proposals in more general asymptotically dS backgrounds. See upcoming work in this direction [30] in the context of extended Schwarzschild-dS

space. Most importantly, one still requires a quantum circuit interpretation to relate the gravitational observables with a proper notion of quantum complexity.

Lastly, we have only investigated the time evolution of complexity in the background geometry without perturbations, however, one of the defining features of holographic complexity is the switchback effect, where one considers how the evolution in the different proposals are modified once shockwave perturbations are introduced. It might be interesting to study this case by sending radial energy pulses from the perspective of the worldline observers and accounting for the backreaction in the geometry (2.8). We hope to study this issue in a future work.

## Acknowledgements

I thank Stefano Baiguera, Mehrdad Mirbabayi, and Nicolò Zenoni for useful discussions and the HECAP group at the International Centre for Theoretical Physics for their hospitality and support during part of the project, and especially my family for hosting me during the preparation of the manuscript. The work of SEAG is partially supported by the FWO Research Project G0H9318N and the inter-university project iBOF/21/084.

## References

- [1] L. Susskind, *Computational Complexity and Black Hole Horizons*, *Fortsch. Phys.* **64** (2016) 24 [[1403.5695](#)].
- [2] D. Stanford and L. Susskind, *Complexity and Shock Wave Geometries*, *Phys. Rev. D* **90** (2014) 126007 [[1406.2678](#)].
- [3] A. Belin, R.C. Myers, S.-M. Ruan, G. Sárosi and A.J. Speranza, *Does Complexity Equal Anything?*, *Phys. Rev. Lett.* **128** (2022) 081602 [[2111.02429](#)].
- [4] A. Belin, R.C. Myers, S.-M. Ruan, G. Sárosi and A.J. Speranza, *Complexity equals anything II*, *JHEP* **01** (2023) 154 [[2210.09647](#)].
- [5] E. Jørstad, R.C. Myers and S.-M. Ruan, *Complexity=anything: singularity probes*, *JHEP* **07** (2023) 223 [[2304.05453](#)].
- [6] S.E. Aguilar-Gutierrez, A.K. Patra and J.F. Pedraza, *Entangled universes in dS wedge holography*, *JHEP* **10** (2023) 156 [[2308.05666](#)].
- [7] S.E. Aguilar-Gutierrez, M.P. Heller and S. Van der Schueren, *Complexity = Anything Can Grow Forever in de Sitter*, [2305.11280](#).
- [8] S.E. Aguilar-Gutierrez, *C=Anything and the switchback effect in Schwarzschild-de Sitter space*, [2309.05848](#).
- [9] L. Susskind, *Entanglement and Chaos in De Sitter Space Holography: An SYK Example*, *JHAP* **1** (2021) 1 [[2109.14104](#)].
- [10] D.A. Galante, *Modave lectures on de Sitter space & holography*, *PoS Modave2022* (2023) 003 [[2306.10141](#)].



- [11] E. Jørstad, R.C. Myers and S.-M. Ruan, *Holographic complexity in  $dS_{d+1}$* , *JHEP* **05** (2022) 119 [[2202.10684](#)].
- [12] R. Auzzi, G. Nardelli, G.P. Ungureanu and N. Zenoni, *Volume complexity of  $dS$  bubbles*, *Phys. Rev. D* **108** (2023) 026006 [[2302.03584](#)].
- [13] T. Anegawa, N. Iizuka, S.K. Sake and N. Zenoni, *Is Action Complexity better for de Sitter space in Jackiw-Teitelboim gravity?*, [2303.05025](#).
- [14] S. Baiguera, R. Berman, S. Chapman and R.C. Myers, *The cosmological switchback effect*, *JHEP* **07** (2023) 162 [[2304.15008](#)].
- [15] T. Anegawa and N. Iizuka, *Shock waves and delay of hyperfast growth in de Sitter complexity*, *JHEP* **08** (2023) 115 [[2304.14620](#)].
- [16] E. Witten, *A Background Independent Algebra in Quantum Gravity*, [2308.03663](#).
- [17] S.E. Aguilar-Gutierrez, *Entanglement and factorization in axion-de Sitter universes*, [2312.08368](#).
- [18] J.B. Hartle and S.W. Hawking, *Wave Function of the Universe*, *Phys. Rev. D* **28** (1983) 2960.
- [19] M. Gutperle and W. Sabra, *Instantons and wormholes in Minkowski and (A)dS spaces*, *Nucl. Phys. B* **647** (2002) 344 [[hep-th/0206153](#)].
- [20] S.E. Aguilar-Gutierrez, T. Hertog, R. Tielemans, J.P. van der Schaar and T. Van Riet, *Axion-de Sitter wormholes*, [2306.13951](#).
- [21] A. Strominger, *The  $dS$  / CFT correspondence*, *JHEP* **10** (2001) 034 [[hep-th/0106113](#)].
- [22] S.B. Giddings and A. Strominger, *STRING WORMHOLES*, *Phys. Lett. B* **230** (1989) 46.
- [23] J. Hartle and T. Hertog, *Arrows of Time in the Bouncing Universes of the No-boundary Quantum State*, *Phys. Rev. D* **85** (2012) 103524 [[1104.1733](#)].
- [24] J.E. Marsden and F.J. Tipler, *Maximal hypersurfaces and foliations of constant mean curvature in general relativity*, *Physics Reports* **66** (1980) 109.
- [25] S. Baiguera, S. Chapman, G. Policastro and T. Schwartzman, *The Complexity of Being Entangled*, [2311.04277](#).
- [26] M.A. Nielsen, *A geometric approach to quantum circuit lower bounds*, *Quantum Info. Comput.* **6** (2006) 213–262.
- [27] M.A. Nielsen, M.R. Dowling, M. Gu and A.C. Doherty, *Quantum computation as geometry*, *Science* **311** (2006) 1133.
- [28] M.R. Dowling and M.A. Nielsen, *The geometry of quantum computation*, *Quantum Information & Computation* **8** (2008) 861.
- [29] S.E. Aguilar-Gutierrez and A. Rolph, *Krylov complexity is not a measure of distance between states or operators*, [2311.04093](#).
- [30] S.E. Aguilar-Gutierrez, S. Baiguera and N. Zenoni, *Holographic complexity of the extended Schwarzschild-de Sitter space*, to appear.